Proceedings of the ASME 2018 International Design Engineering Technical Conferences & Computers and Information in Engineering Conference
IDETC2018
August 26–29, 2018 in Quebec City, Canada

IDETC2018-85506

DESIGN AUTOMATION BY INTEGRATING GENERATIVE ADVERSARIAL NETWORKS AND TOPOLOGY OPTIMIZATION

Sangeun Oh
K-School
Korea Advanced Institute of Science and Technology
Daejeon, South Korea
e-mail: aeroplan@kaist.ac.kr

Yongsu Jung
Mechanical Engineering
Korea Advanced Institute of Science and Technology
Daejeon, South Korea
e-mail: yongsu50@kaist.ac.kr

Ikjin Lee
Mechanical Engineering
Korea Advanced Institute of Science and Technology
Daejeon, South Korea
e-mail: ikjin.lee@kaist.ac.kr

Namwoo Kang*
Mechanical Systems Engineering
Sookmyung Women's University
Seoul, South Korea
e-mail: nwkang@sm.ac.kr

ABSTRACT

Recent advances in deep learning enable machines to learn existing designs by themselves and to create new designs. Generative adversarial networks (GANs) are widely used to generate new images and data by unsupervised learning. Certain limitations exist in applying GANs directly to product designs. It requires a large amount of data, produces uneven output quality, and does not guarantee engineering performance. To solve these problems, this paper proposes a design automation process by combining GANs and topology optimization. The suggested process has been applied to the wheel design of automobiles and has shown that an aesthetically superior and technically meaningful design can be automatically generated without human interventions.

NOMENCLATURE

$\mathbb{E}$: expectation
D: differentiable function of discriminator
G: differentiable function of generator
z: noise variable
$\mathcal{L}$: loss function of auto-encoder
c: compliance
x_e: density variable
$\tilde{x}_e$: filtered density variable
$\bar{\tilde{x}}_e$: projected density variable
p: penalization factor

1. INTRODUCTION

Artificial intelligence (AI) pursues machines to have human intelligence. Machine learning attempts computers to acquire their own knowledge by extracting features from raw data. With a nested hierarchical structure represented from deep graphs that consist of many layers, deep learning tries to enhance the learning ability of the computer system in a supervised and an unsupervised manner [1]. Generative adversarial networks (GANs) are deep generative models that belong to unsupervised learning [2]. They produce images from the learning and have training images as inputs. Thus, they are widely used in areas requiring creativity, such as art and design [3, 4].

GANs are a zero-sum game between two players, generators, and discriminators. A generator produces a fake sample and sends it to a discriminator. Given the data from a training set and from the generator, the discriminator determines which data are real and which are fake (see Figure 1). Thus, the competition framework with the conflicting goals of two players generates a process of raising one's ability and offsetting the counterpart's capacity. This process leads GANs to reach an equilibrium state where the discriminator cannot determine real and fake samples and consistently emits a 0.5 probability [2]. Image data generated by GANs at this point are also plausible for humans to believe as real ones imply that product design is no longer restricted to humans alone.

However, certain limitations in using GANs directly for autonomous design are found. (1) Gathering large amounts of data enough to train a model is difficult. Training with a neural network generally recommends having at least five million data [2] Considerable research uses more than 10 million data. Collecting such amount of data of the same product design is a challenging task. (2) GANs do not guarantee the production of image data of robust quality. Depending on the quantity and quality of training data, the output quality of a training model varies. Figure 2 shows that the difference among design quality generated from the same model state also exists. (3) As GANs learn by training an existing design and create a new design by making a small change within that design space, output from GANs can be aesthetically satisfiable but cannot be meaningful in engineering. For this reason, directly adopting images generated from GANs to products requiring engineering performance and safety is rarely possible.

* Address all correspondence to this author.

The proposed research combines GANs and topology optimization to make up for the weakness of GANs. Topology optimization is a computational material distribution method within a prescribed design domain.

Figure 1. While the generator seeks to create a sample making the discriminator to regard it as data from the training set, the discriminator tries to make a right judgment about the data's origin. Gray boxes represent the inputs, and white ones represent outputs.

Therefore, it can freely find high-performance structure layouts. In this study, the compliance minimization problem, which is the most basic and general problem in topology optimization, is formulated and applied to a two-dimensional wheel design. Moreover, the density approach, which is one of the approaches in topology optimization, is used. Therefore, the objective function is the compliance of wheel while maintaining the given volume fraction, and the design variable of optimization is element-wise density that is expected to converge to zero as void or one as solid. However, the design obtained from topology optimization is concentrated on the prescribed engineering performance. Thus, it sometimes produces weird designs. The weird design means that it did not take into account the aesthetic characteristics which is the important to customers. Sometimes, the aesthetic things of the design does not matter, but the wheel is not. In product design, a good design should not only be satisfied in performance but also be perceived as realistic and aesthetic. Although certain research proposed additional strategies to consider the manufacturability, the aesthetic aspect cannot be managed by formulation easily.

In this study, we propose a design automation process, which creates an initial product design with GANs and then complements it by topology optimization. This process provides a design with excellent engineering performance. Without any human intervention, this AI system can make an aesthetic design similar to existing ones, which have technical features with high performance in large quantities. Designers can select from design options generated by the proposed process and acquire new design insights. Furthermore, creating an infinite number of new designs is theoretically possible. Moreover, all designs achieve an exceptional engineering performance. Thus, we apply this methodology to car wheel designs.

The rest of this paper is structured as follows. Section 2 introduces studies using deep learning in engineering design, GANs and topology optimization. Section 3 suggests a design automation process. Section 4 analyzes and discusses the results. Finally, Section 5 summarizes the conclusions and introduces future work.

2. RELATED WORK

2.1. DEEP LEARNING IN ENGINEERING DESIGN

There have been many efforts related to deep learning in the engineering design community in accordance with AI development. Studies training product images and attributes simultaneously through deep neural networks have shown that they can identify various potential design spaces in product form and analyze and predict the aesthetic design characteristics perceived by customers in heterogeneous markets. This allows designers to explore new design possibilities or see if a given design achieves intended aesthetic design features [5,6]. In addition, there is a study about improving prediction accuracy of customer's preference model by learning Restricted Boltzmann machine with the original design variables as input and extracting the futures. It shows using deep neural network has higher prediction accuracy than the existing models without the feature learning [7]. Besides to predicting customer preferences about design, research has also been done to map the form and function of the design. Using 3D convolution neural network, it learned to map the form and function of an object, making it possible to predict the function given the form of the object. This research of prediction about form and function presented the possibility that the prediction of product function based on the form can be made automatically without human interventions [8]. Also, the image generation model that integrates deep learning and big data and its utility have been studied [9].

While there have been various efforts in the field of engineering design using deep learning, many of them focus on improving prediction accuracy on design related problems and there is a little research on automated design creation. Therefore, this study proposes a methodology of product design generation that both minimizes human interventions and guarantees engineering performance.

2.2. GANS

GANs are designed to infer the data generating distribution $p_{\mathbf{data}}(x)$ by making the model distribution generated by generator $p_{\mathbf{g}}(G)$ to be close to the real data distribution where x is the variable of real data and G is the generator's differentiable function with parameters $\theta_{\mathbf{g}}$. Function G has an input noise variable z and tries to map it to the real data space by adjusting $\theta_{\mathbf{g}}$, thus represented as $G(z;\theta_{\mathbf{g}})$. Similarly, the discriminator's differentiable function is derived as $D(x;\theta_{\mathbf{d}})$, which outputs of the probability certain data are from the training dataset. The zero-sum game of maximizing the discriminator and generator is equivalent to maximizing $\log D(x)$ and minimizing $\log(1-D(G(z)))$ [10, 11].

$$\min_G \max_D V(D,G) = \mathrm{E}_{x\sim p_{data}(x)}[\log D(x)] + \mathrm{E}_{z\sim p_z(z)}[\log(1-D(G(z))] \quad (1)$$

With this standard GAN structure, various GANs have been developed by modifying the generator, discriminator, or objective function.

Figure 2. Generated faces after 240,000 iterations with randomly selected 2,000 CelebA dataset by boundary equilibrium GANs (BEGANs) [16]. A few distorted faces are created with normal-looking faces.

To overcome the notorious difficulty in training GANs, deep convolutional GANs (DCGANs) provide a stable training model, which works on various datasets by constructing a convolutional neural network in the generator and discriminator. In addition, DCGANs suggest certain techniques such as removing a fully-connected layer on

top, applying batch normalization, and using the leaky rectified linear unit activation function [12]. Adversarially learned inference (ALI) and bidirectional GANs (BiGANs) adopt the encoding–decoding model to the generator to improve the quality of generated samples in an efficient way. Moreover, BiGANs emphasize taking advantages of learned features [13, 14]. For high-resolution images with stable convergence and scalability, energy-based GANs (EBGANs) have proven to produce realistic 128 × 128 images. EBGANs consider the discriminator as an energy function and the energy as the reconstruction error. From this point of view, an auto-encoder architecture is used for the discriminator [15]. The auto-encoder consists of encoder and decoder functions. The input value is transformed through the encoder and is restored to its original form again through the decoder [1]. Wasserstein GANs (WGANs) approach the way to obtain good image quality by changing the distance measure of two probability distributions. WGANs show that the earth-mover distance, which is also called Wasserstein-1, provides a differentiable function, and, thus, produces meaningful gradients, whereas Kullback-Leibler and Jensen-Shannon divergence in previous research do not when two probability distributions are disjointed [11]. Boundary Equilibrium GANs (BEGANs) also use the Wasserstein distance as a measure of convergence. BEGANs present an equilibrium concept, balancing the discriminator and generator in training and the numerical way of global convergence [16].

Aside from enhancing the image quality, the way to control the mode of generated outputs is presented by convolutional GANs (cGANs) and InfoGAN(Information maximizing Generative Adversarial Nets). cGANs provide additional input values to the generator and discriminator for categorical image generation. Furthermore, InfoGAN lets the generator produce uncategorical images by adding a latent code that can be categorical and continuous [17, 18]. It is useful for finding hidden representations from large amounts of data. However, intentionally creating a specific image is still difficult.

Hitherto, many studies on GANs contribute to good image quality in terms of convergence and stability. However, GANs are still weak in utilizing from the design engineering point of view, such as uneven image quality from the same saving point of model, especially when relatively small amounts of training data are given and images have insufficient engineering features.

2.3. TOPOLOGY OPTIMIZATION

Topology optimization is commonly referred to as the material distribution method developed and spread to a wide range of disciplines. [19–21]. The basic concept is how to distribute materials in a given design domain without any preconceived design. In this study, the compliance minimization related to the stiffness of structure is carried out to the design wheel. Furthermore, many approaches, such as homogenization and level-set, can be used, but we use the density-based approach where material distribution is parametrized by the density of elements. Furthermore, solid isotropic material with penalization (SIMP) is a procedure that implicitly penalizes intermediate density values to lead to the black-and-white design. The basic formulation of SIMP in compliance minimization can be written as [21, 22]

$$\begin{aligned} \min \quad & c(\mathbf{x}) = \mathbf{U}^T\mathbf{K}\mathbf{U} = \sum_{e=1}^{NE} \mathbf{u}_e^T (E_e(x_e)\mathbf{k}_0)\mathbf{u}_e \\ \text{s.t} \quad & V(\mathbf{x})/V_0 = f \\ & \mathbf{K}\mathbf{U} = \mathbf{F} \\ & 0 \le x_e \le 1, \ e = 1,\ldots,NE \end{aligned} , \tag{2}$$

where $\mathbf{U}$ is a displacement vector; $\mathbf{K}$ is a global stiffness matrix; $c(\mathbf{x})$ is the compliance; $\mathbf{u}_e$ is an element displacement vector; $\mathbf{k}_0$ is an element stiffness matrix; f is the volume fraction; NE is the number of elements; x_e is the design variable (i.e., density) of element e; and $V(\mathbf{x})$ and V_0 are the material volume and design domain volume, respectively. In modified SIMP, the density is associated with Young's modulus expressed as [23]

$$E_e(x_e) = E_{\min} + x_e^p (E_0 - E_{\min}) , \tag{3}$$

where p is a penalization factor to ensure the black-and-white design, and $E_{\min}$ is introduced to avoid numerical instability when the density of elements become zero.

Many studies have been done to enhance the topology optimization performance such as filtering techniques. In this study, we develop the code based on 99- and 88-line MATLAB codes, which are the most simple and efficient two-dimensional topology optimization codes written in MATLAB [22, 24]. Furthermore, we include the improved techniques developed recently such as a projection filter. Thus, we briefly explain algorithms such as sensitivity analyses and filtering techniques used in this study.

The sensitivity analysis of objective and constraint functions with respect to each design variable is required for gradient-based optimization. It can be given by the following formula:

$$\begin{aligned} \frac{\partial c}{\partial x_e} &= -p x_e^{p-1}(E_0 - E_{\min})\mathbf{u}_e^T\mathbf{k}_0\mathbf{u}_e \\ \frac{\partial V}{\partial x_e} &= \frac{\partial}{\partial x_e}\left(\sum_{e=1}^{NE} x_e v_e - V\right) = 1 \end{aligned} , \tag{4}$$

with the assumption that all elements have a unit volume. The optimality criteria (OC) method, one of the classical approaches to structural optimization problems, is used. The OC method updates the design domain as

$$x_e^{new} = \begin{cases} \max(0, x_e - m) & \text{if } x_e B_e^\eta \le \max(0, x_e - m) \\ \min(1, x_e + m) & \text{if } x_e B_e^\eta \ge \min(1, x_e + m) \\ x_e B_e^\eta & \text{otherwise} \end{cases} , \tag{5}$$

where m is a positive move-limit and η is a numerical damping coefficient

$$B_e = \frac{-\dfrac{\partial c}{\partial x_e}}{\lambda \dfrac{\partial V}{\partial x_e}} \tag{6}$$

The Lagrange multiplier related to volume fraction constraint can be obtained from a bisection algorithm which is one of the popular root-finding algorithms. The termination criteria for the convergence can be written as follows:

$$\left\| \mathbf{x}_{new} - \mathbf{x} \right\|_\infty \le \varepsilon , \tag{7}$$

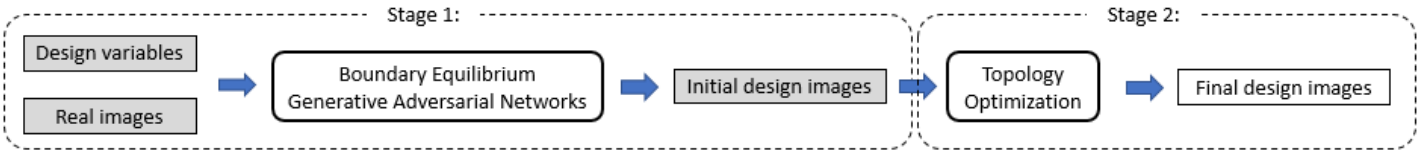

Figure 3 Overview of the design automation system with GANs and topology optimization. Gray boxes represent the inputs, and white ones represent outputs. Initial design images are used as the outputs of GANs and inputs of topology optimization.

where ε is the tolerance usually set as a relatively small value such as 0.01.

For the assurance of the existence of well-posed and mesh-independent solutions, several strategies to avoid a checker-board pattern or gray-scale issue are introduced. In this study, we apply the so-called three-field SIMP, which has a projection scheme [25]. Three-field pertains to the design variable and filtered and projected fields. Detailed description is shown in the literature. We only focus on which method is used in this study because the contribution of the proposed method is the application of topology optimization on the results of the machine learning algorithm.

The basic filters applied to topology optimization are sensitivity and density filters, which are used in one-field SIMP and two-field SIMP, respectively. The main idea of both techniques is to define sensitivity or physical element density to be a weighted average of neighborhood. The neighborhood is defined on the basis of distance from the center of the element, and the maximum distance to include in neighborhood is a user-specified parameter referred to as mesh-independent radius. The sensitivity filter can be written as [26]

$$\frac{\partial c}{\partial x_e} = \frac{1}{x_e \sum_{f=1}^{N} H_f} \sum_{f=1}^{N} H_f x_f \frac{\partial c}{\partial x_f}, \tag{8}$$

where the convolution operator can be written as follows:

$$H_f = r_{\min} - \mathrm{dist}(e, f), \tag{9}$$

where subscript f means one of the elements that the center-to-center distance expressed as $\mathrm{dist}(e, f)$ between elements is smaller than $r_{\min}$.

The density filter defines the physical density with weighted averaging. The weighted average concept is the same in the sensitivity filter as Eq. (8), but the density is filtered instead of sensitivity expressed as [27, 28]

$$\tilde{x}_e = \frac{\sum_{f=1}^{N} H_f x_f}{\sum_{f=1}^{N} H_f} \tag{10}$$

Therefore, original and filtered densities can be referred to as a design variable and physical density, respectively. The sensitivity analysis with respect to design variables should be modified by introducing the physical density using a chain rule. A detailed description can be seen in the literature.

The weighted average is used in both filtering methods to avoid the checker-board pattern in an optimum design. However, the density filter can induce gray transitions between solid and void regions. Thus, the third field of density, or the so-called projection filter, is introduced. It mitigates the gray transition problem by projecting to solid and void usually using a smoothed Heaviside projection [23, 29, 30]. In this study, we use the Heaviside projection filter on the filtered density obtained from Eq. (10). The projection filter can be written as follows:

$$\bar{\tilde{x}}_e = 1 - e^{-\beta \tilde{x}_e} + \tilde{x}_e e^{-\beta}, \tag{11}$$

where β is a parameter related to slope of projection and can be updated through the optimization. In three-field SIMP with projection filter, the sensitivity analysis is modified compared with Eq. (8) because the finite element analysis is performed on the basis of the physical density obtained from Eq. (11). The sensitivity analysis with respect to design variables can be easily derived using the chain rule.

Many studies have been done to avoid problems occurring in topology optimization as mentioned hitherto. In this study, we use the Heaviside projection filter in accordance with post-processing. The objective of topology optimization in the entire methodology is to enhance the engineering performance of various designs obtained from GANs. Therefore, we do not perform the topology optimization in a common way. The design space is restricted in the void region of design from GANs. It will be explained in the next section

3. PROPOSED DESIGN AUTOMATION

We propose a design automation approach, which integrates GANs and topology optimization. This process consists of two stages. Figure 3 shows the entire process. Stage 1 creates images from training BEGANs. Stage 2 uses the images from stage 1 as the inputs of topology optimization. Through the process of topology optimization, images from GANs are translated to those that satisfy technical requirements.

3.1. STAGE 1: GENERATING AN AESTHETIC DESIGN BY GANS

BEGANs provide a robust visual quality in a fast and stable manner. The auto-encoder architecture as the discriminator used in EBGANs is also introduced by BEGANs. Similar to WGANs, BEGANs use the Wasserstein distance as a measure of convergence. With these techniques, BEGANs achieve reliable gradients that are difficult for high-resolution 128 × 128 images.

Rather than trying to match the probability distribution of real data, BEGANs focus on matching auto-encoder loss distribution. It measures the loss, which is the difference between the sample and its output that passed through the auto-encoder. Subsequently, a lower bound of the

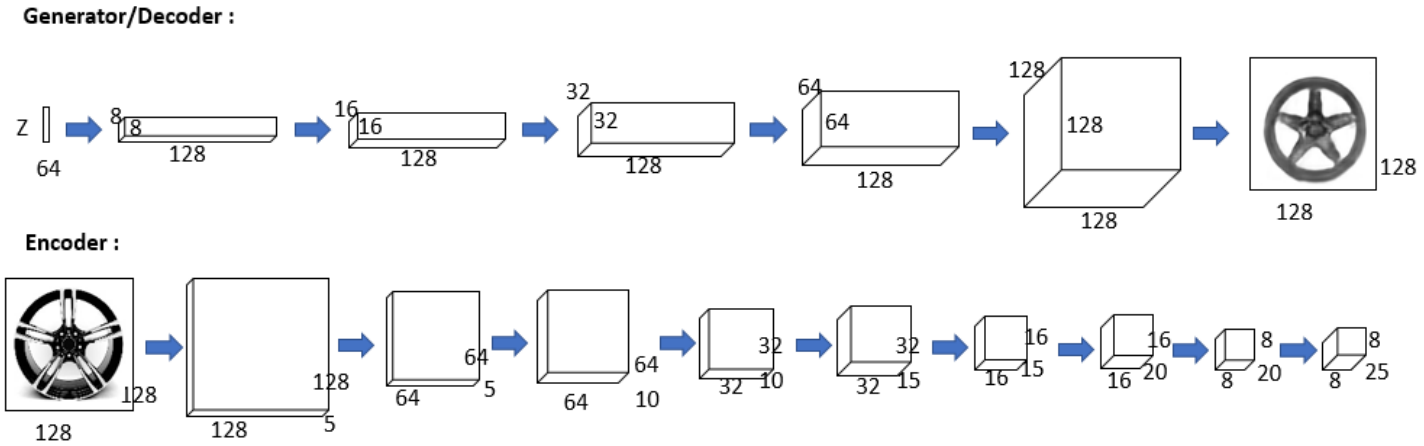

Figure 4. Network architecture of the training model

Wasserstein distance between the auto-encoder loss distribution of real and that of generated samples is derived. The auto-encoder loss function, $\mathcal{L}: \mathbb{R}^{N_x} \rightarrow \mathbb{R}^{+}$, is defined as the following.

$$\mathcal{L}(v) = |v - A(v)|^{\eta}$$

where

$$\begin{cases} A: \mathbb{R}^{N_x} \rightarrow \mathbb{R}^{N_x} & \text{is an autoencoder function.} \\ \eta \in \{1,2\} & \text{is a target norm.} \\ v \in \mathbb{R}^{N_z} & \text{is a sample of dimension } N^z. \end{cases} \quad (12)$$

Applying Jensens's inequality, the lower bound of the Wasserstein distance is derived as the following.

$$|m_1 - m_2| \quad (13)$$

where $m_i \in \mathbb{R}$ is the mean of auto-encoder loss distribution. For the maximization of Eq. (13) for the discriminator with $m_1 \rightarrow 0$ and $m_2 \rightarrow \infty$, BEGANs' objective function is described as minimizing the discriminator's auto-encoder loss function $\mathcal{L}_D$ and generator's one $\mathcal{L}_G$ as the following where θ_D and θ_G are the parameters of the discriminator and generator, $G: \mathbb{R}^{N_z} \rightarrow \mathbb{R}^{N_z}$ is the generator function, $z \in [-1,1]^{N_z}$ are uniform random samples of dimension N_z, and z_D and z_G are samples form z.

$$\begin{cases} \mathrm{L}_D = \mathrm{L}(x) - k_t \mathrm{L}(G(z_D)) \quad \text{for} \quad \theta_D \\ \mathrm{L}_G = \mathrm{L}(G(z_G)) \quad \text{for} \quad \theta_G \\ k_{t+1} = k_t - \lambda_k(\gamma \mathrm{L}(x) - \mathrm{L}(G(z_G))) \quad \text{for} \quad \gamma = \dfrac{\mathrm{E}[\mathrm{L}(G(z))]}{\mathrm{E}[\mathrm{L}(x)]} \end{cases} \quad (14)$$

where $k_t \in [0,1]$ is a control factor to determine how much $\mathcal{L}(G(z_D))$ is reflected during gradient descent; λ_k is a proportional gain for k such as the learning rate in machine learning terms; and $\gamma \in [0,1]$ is a diversity ratio that results in high image diversity as it increases. Given that k_t is changed every training step to maintain $\mathbb{E}[\mathcal{L}(G(z))] = \gamma\mathbb{E}[\mathcal{L}(x)]$ for the equilibrium, global measure of convergence is regarded as the closest reconstruction $\mathcal{L}(x)$ with minimum absolute value of proportional control algorithm error $|\gamma\mathcal{L}(x) - \mathcal{L}(G(z_G))|$ [16].

$$M_{global} = \mathrm{L}(x) + |\gamma(\mathrm{L}(x)) - \mathrm{L}(G(z_G))| \quad (15)$$

The model trained in our research has a network architecture that only consists of the nearest neighbor up-sampling and 3 × 3 convolutions with stride 2 for down-sampling and the exponential linear unit activation function. Figure 4 illustrates this architecture. We use the Adam optimizer with a learning rate of 0.00008, initial value of k_t as 0, λ_k as 0.001, γ for 0.7, and minibatch size of 16. The learning rate parameter is set with reference to the settings of papers that studied image quality using BEGAN [31, 32]. Given that the number of training dataset is 1,728, the training takes a few hours on a single GTX 1080 GPU.

Figure 5 presents 128 × 128 images from the BEGAN generator, and Figure 6 describes its global convergence showing $\mathcal{M}_{global} \approx \mathcal{L}(x)$. We focus on obtaining realistic images that have symmetrical spokes connected to a rim and hub. From the output images, these wheel constraints may seem to be met by humans. However, certain images illustrated with brightness are considered disconnected by the machine. In addition, some images clarify wheel studs, whereas others do not. Thus, the image quality is not uniform.

For generating machine readable wheel images, certain limitations for gathering suitable data exist. We only gather images containing one wheel and a white-colored background to make the machine assign black for wheel and white for the rest. In addition, most wheel sites offer pictures of wheels tilted at an angle to show their width. Such pictures make the dataset small. As the images containing only the front aspect of wheels are interpretable for the machine to compute the engineering performance, many data with wheels' side aspect are eliminated from the dataset, which implies that gathering enough training dataset of engineering design is a challenging task. Despite the scarce data of only 1,728 training datasets, BEGANs produce reliable wheel images. However, it struggles to provide equivalent image quality because of the insufficient training dataset.

Figure 5. 128 × 128 wheel designs after 240,000 iterations by BE-GANs

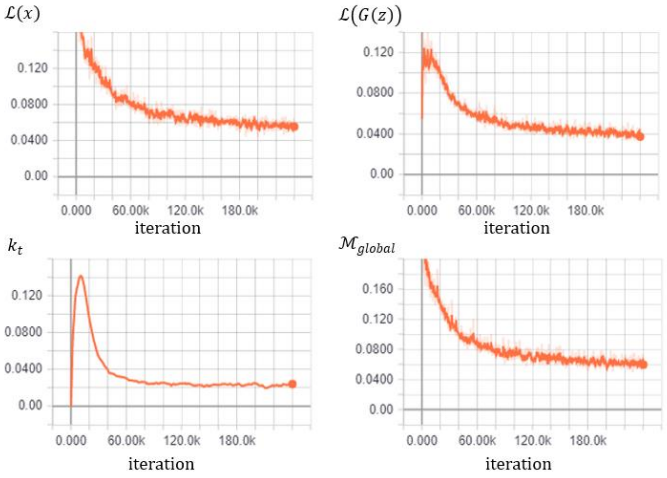

Figure 6. With γ as 0.7, auto-encoder loss of the discriminator (upper left), auto-encoder loss of the generator (upper right), k_t (lower left), and $\mathcal{M}_{global}$ (lower right)

3.2. STAGE 2: ENHANCING ENGINEERING PERFORMANCE BY TOPOLOGY OPTIMIZATION

Designs from GANs are aesthetic because they are generated on the basis of the database of existing man-designed wheels. These designs may not make people feel the sense of difference if no problem arises in the image resolution or structure infeasibility. However, designs obtained from GANs can be generally infeasible due to poor engineering performance, which is totally ignored in producing new designs.

Designs obtained from GANs should go through the post-processing by either algorithms or human because certain imperfect designs exist. Therefore, the topology optimization is applied to the proposed methodology in the post-processing to enhance engineering performance. Through the post-processing with topology optimization, designs obtained from GANs can be complete as almost binary 0-1 designs, which means solid or void materials in each element. Moreover, the topology optimization can guarantee the feasibility in engineering performance. The matter is how to apply the topology optimization in the post-processing of designs obtained from GANs while maintaining the originality in shape.

In this study, we apply the topology optimization in a different way. A design domain is restricted in the void region of the initial design called a predefined domain by GANs. The topology optimization in the entire design domain setting the initial design as a design obtained from GANs makes a totally different design from the initial one. Such difference is against the purpose of post-processing, which improves the engineering performance while maintaining the initial design. Figure 7 sketches the design domain and boundary condition of the two-dimensional wheel design [33, 34]. The original design domain is 128 x 128 elements given that the images obtained from GANs have 128 x128 pixels. Thus, the cut outer region of the wheel is a non-design region. The outer boundary of the wheel is also a non-design region to treat as the rim. The fixed boundary condition is applied to an inner ring. The element stiffness matrix is based on a 4-node bi-linear square element in the 88-line topology optimization MATLAB code. The material is defined as a common steel.

The load conditions are simple. The normal and shear forces are uniformly exerted on a surface, following the outer boundary of the design domain that is the circumference of the outer circle. The following are common conditions in the two-dimensional wheel design. The normal force is referred to as a uniform tire pressure, and the shear force is referred to as a uniform tangential traction. We do not consider the ground reaction induced by vehicle weight usually treated as cosine function for simplicity.

The most important thing is the cyclic symmetry of the wheel design. Given that we perform the topology optimization based on MATLAB codes and finite element analyses for well-continuity with GANs, all meshes are square. Images obtained from GANs also consist of square pixels. However, achieving the cyclic symmetry of the wheel can be a problem. The square meshes parallel with x and y axes do not satisfy the cyclic symmetry. Thus, we add a cyclic symmetry condition based on the unit cell concept that is duplicated with rotation.

As mentioned above, setting the design obtained from GANs as the initial design results in a totally different design that is against the purpose of post-processing. Although the optimum in topology optimization is fairly a high-quality design, it is far from the initial design. The engineering performance may be enhanced, but it loses the specialty of GANs. Thus, we restrict the design domain as the void region of designs from GANs to add reinforcement in the structure and enhance the stiffness. Figure 8 illustrates the restricted design domain for topology optimization with and without cyclic symmetry conditions.

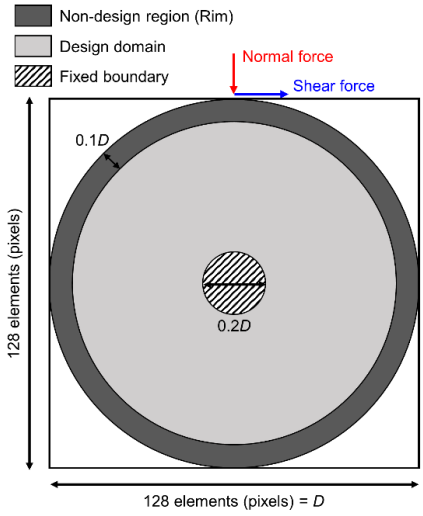

Figure 7. Design domain and boundary condition of a 2D wheel design

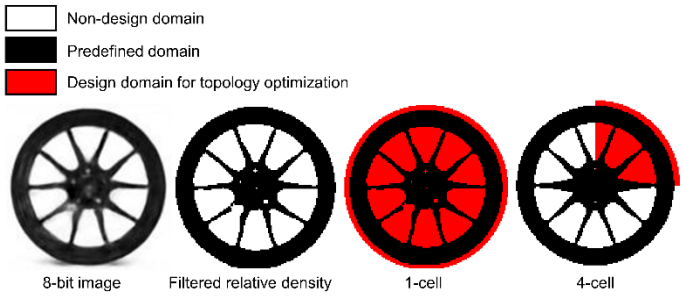

Figure 8. Restricted design domain

In Figure 8, the restricted design domain is described with the cyclic symmetry condition, especially the 4-cell design. The design domain for the cyclic condition has a red color, and it is decided by the predefined domain by GANs. The inner ring and rim constraints are omitted in Figure 8. The cyclic condition is not limited to the design domain but is extended to the predefined domain. The cyclic symmetry condition is a necessary condition of the wheel design due to the stability and durability of structure. However, the initial design obtained from GANs may not have a cyclic symmetric design. Results affected by this additional condition can be seen in the 4-cell design in Figure 9.

Therefore, several parameters are introduced for post-processing using topology optimization. First, the threshold for conversion from 8-bit image to the binary design is introduced. Given that the design obtained from GANs is an 8-bit image, the threshold is necessary to convert it to the perfect solid of the void design. The initial volume fraction automatically decides which is specified by a user. Second, the additional volume fraction is introduced. It is the reinforcement volume in the restricted design domain for topology optimization. Third, the number of unit cells should be decided. In addition, the cyclic symmetry is necessary to the design wheel. The process of post-processing using topology optimization is illustrated in Figure 9 with an example.

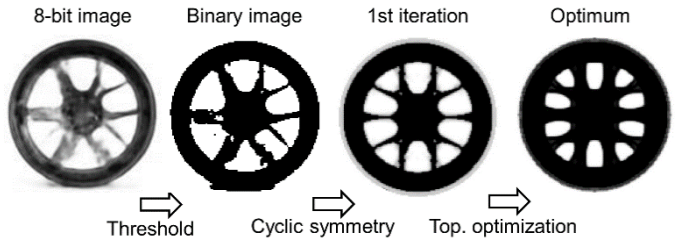

Figure 9. Post-processing using topology optimization

From the left initial image, the engineering performance of design, which is the compliance in this paper, is improved, and the design becomes clearer than the initial unclear image due to density and Heaviside projection filtering techniques.

Figure 10 exhibits the effect of the predefined design domain. The optimum image is fairly different without the predefined image only using the 8-bit image as the initial design of topology optimization. Optimum images with or without cyclic symmetry preserved the original image while enhancing the engineering performance. The design referred to as no predefined is the optimum from the initial GAN design without a predefined domain and cyclic symmetry. The predefined and 1-cell means the optimum with predefined design and no cyclic symmetry due to a one-unit cell. Figure 11 shows the engineering performance of various designs during topology optimization. Therefore, the initial design which denoted as the first iteration in Figure 11 is obtained from GAN. The compliance of design with the proposed method is larger than images with no predefined domain, but it lost originality in design. In the convergence history, the small increasing in compliance is due to modification of filtering parameter in Eq. (11), and it is also exaggerated because of log-scale. It is natural convergence history when projected filtering is used.

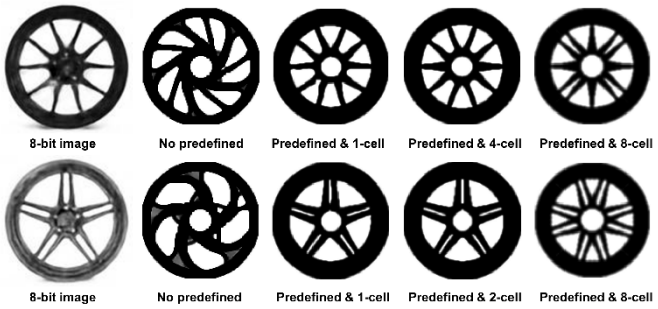

Figure 10. Result with and without predefined image

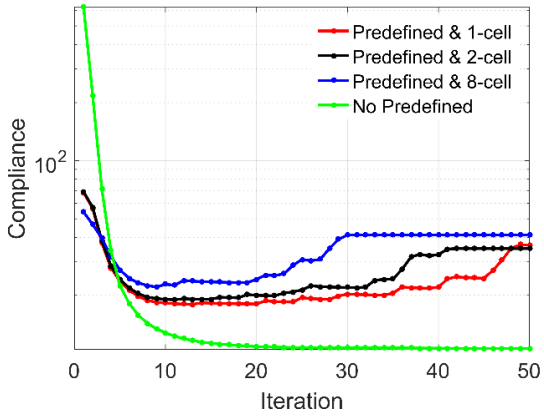

Figure 11. Compliance between various optimum designs

Pointing out that the final design after post-processing can maintain the basic shape of the initial design due to the restricted design domain is important.

4. RESULTS

In this section, various images obtained from GANs and the final design post-processed by topology optimization are shown in Figure 12. All parameters applied to each optimization are similar. The initial volume fraction from GANs is 0.4, and the additional volume fraction is 0.2. Thus, the finalized volume fraction is 0.6.

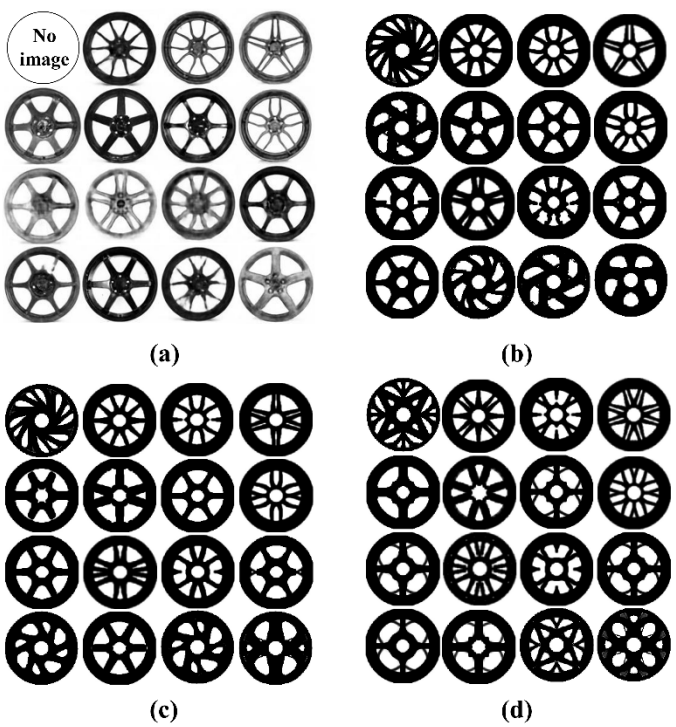

Figure 12. (a) Initial images and modified designs using topology optimization with (b) 2-cell, (c) 4-cell, and (d) 8-cell

In Figure 12, three cases are categorized with the number of cells. The number of cells means the portion of the cyclic symmetry. The 2-cell means that 1/2 of design domain is optimized and the remaining part duplicate it. Likewise, the 4-cell condition means 1/4 of design domain is optimized through topology optimization and remaining parts will be filled with optimized 1/4 part based on cyclic symmetry. It can be easily checked in the results. The cyclic symmetry is applied in two ways depending on how it rotates, and we choose it manually. Various wheel designs are produced through post-processing, and certain images appear to be weird and infeasible compared with original images even if compliances are enhanced. The reason is that the optimum designs from topology optimization strongly depend on parameters such as beta for the projection filter, initial and additional volume fractions, and the ratio of two forces (i.e., normal and shear). Therefore, consistently generating good designs with fixed parameters is difficult, and ongoing research developing robust and creative ways to combine GANs and topology optimization is necessary. The study aims to generate various feasible wheel designs combining GANs and topology optimization, and we attained it as seen in Figure 12.

5. CONCLUSION

As AI develops, the generative model from deep learning presented the possibility that machines can be designers. However, many restrictions in using outputs from the generative model as the final designs of products still exist given that such outputs must meet engineering performance requirements. We use topology optimization to compensate for these drawbacks and introduced a design automation process integrating GANs and topology optimization. The suggested methodology has proved that it can produce aesthetically and technically superior designs without being significantly affected by image quality from GANs. Thus, the outputs of GANs with a relatively small amount of input data become meaningful.

In our future work, we will develop a design automation process that can additionally learn engineering designs by conducting an iterative process of learning designs created again by topology optimization with GANs.

ACKNOWLEDGMENTS

This work was partially supported by the National Research Foundation of Korea (NRF) and grant funded by the Korea government (N01170150). This support is gratefully acknowledged.

REFERENCES

[1] Goodfellow, I., Bengio, Y. & Courville, A., 2016, “Deep Learning,” The MIT Press, pp. 1-8.

[2] Goodfellow, I., 2016, “NIPS 2016 Tutorial: Generative Adversarial Networks,” *arXiv:1071.00160 [cs]*, Dec.

[3] Elgammal, A., Liu, B., Elhoseiny, M., & Mazzone, M., 2017, “CAN: Creative Adversarial Networks, Generating "Art" by Learning About Styles and Deviating from Style Norms,” *arXiv:1706.07068 [cs]*, Jun.

[4] Wu, J., Zhang, C., Xue, T., Freeman, W. T., & Tenenbaum, J. B., 2016, “Learning a Probabilistic Latent Space of Object Shapes via 3D Generative-Adversarial Modeling,” *arXiv:1610.07584 [cs]*, Otc.

[5] Burnap, A., Liu, Y., Pan, Y., Lee, H., Gonzalez, R., & Papalambros, P. Y., 2016, “Estimating and exploring the product form design space using deep generative models,” In ASME International Design Engineering Technical Conferences and Computers and Information in Engineering Conference, American Society of Mechanical Engineers, pp. V02AT03A013-V02AT03A013

[6] Pan, Y., Burnap, A., Hartley, J., Gonzalez, R., & Papalambros, P. Y., 2017, “Deep Design: Product Aesthetics for Heterogeneous Markets,” In Proceedings of the 23rd ACM SIGKDD International Conference on Knowledge Discovery and Data Mining, ACM, pp. 1961-1970

[7] Burnap, A., Pan, Y., Liu, Y., Ren, Y., Lee, H., Gonzalez, R., & Papalambros, P. Y., 2016, “Improving design preference prediction accuracy using feature learning,” Journal of Mechanical Design, 138(7), 071404

[8] Dering, M. L., & Tucker, C. S., 2017, “A Convolutional Neural Network Model for Predicting a Product's Function, Given Its Form”, Journal of Mechanical Design, 139(11), 111408

[9] Dering, M. L., & Tucker, C. S., 2017, “Generative adversarial networks for increasing the veracity of big data,” In Big Data (Big Data), 2017 IEEE International Conference, IEEE, pp. 2595-2602

[10] Goodfellow, I. J., Pouget-Abadie, J., Mirza, M., Xu, B., Warde-Farley, D., Ozair, S., Courville, A., & Bengio, Y., 2014, “Generative Adversarial Networks,” *arXiv:1406.2661 [cs]*, Jun.

[11] Arjovsky, M., Chintala, S., & Bottou, L., 2017, “Wasserstein GAN,” *arXiv:1701.07875 [cs]*, Jan.

[12] Radford, A., Metz, L., & Chintala, S., 2015, “Unsupervised Representation Learning with Deep Convolutional Generative Adversarial Networks,” *arXiv:1511.06434 [cs]*, Nov.

[13] Dumoulin, V., Belghazi, I., Poole, B., Mastropietro, O., Lamb, A., Arjovsky, M., & Courville, A., 2016, “Adversarially Learned Inference,” *arXiv:1606.00704 [cs]*, Jun.

[14] Donahue, J., Krähenbühl, P., & Darrell, T., 2016, “Adversarial Feature Learning,” *arXiv:1605.09782 [cs]*, May.

[15] Zhao, J., Mathieu, M., & LeCun, Y., 2016, "Energy-based Generative Adversarial Network," *arXiv:1609.03126 [cs]*, Sep.
[16] Berthelot, D., Schumm, T., & Metz, L., 2017, "BEGAN: Boundary Equilibrium Generative Adversarial Networks," *arXiv:1703.10717 [cs]*, Mar.
[17] Mirza, M., & Osindero, S., 2014, "Conditional Generative Adversarial Nets," *arXiv:1411.1784 [cs]*, Nov.
[18] Chen, X., Duan, Y., Houthooft, R., Schulman, J., Sutskever, I., & Abbeel, P., 2016, "InfoGAN: Interpretable Representation Learning by Information Maximizing Generative Adversarial Nets," *arXiv:1606.03657 [cs]*, Jun.
[19] Bendsøe, M. P., & Kikuchi, N., 1988, "Generating optimal topologies in structural design using a homogenization method," Computer methods in applied mechanics and engineering, 71(2), 197-224.
[20] Bendsøe, M. P., 1989, "Optimal shape design as a material distribution problem," Structural optimization, 1(4), 193-202
[21] Bendsøe, M. P., & Sigmund, O., 2013, "Topology optimization: theory, methods, and applications," Springer Science & Business Media.
[22] Sigmund, O., 2001, "A 99 line topology optimization code written in Matlab. Structural and multidisciplinary optimization," 21(2), 120-127.
[23] Sigmund, O., 2007, "Morphology-based black and white filters for topology optimization," Structural and Multidisciplinary Optimization, 33(4-5), 401-424.
[24] Andreassen, E., Clausen, A., Schevenels, M., Lazarov, B. S., & Sigmund, O., 2011, "Efficient topology optimization in MATLAB using 88 lines of code," Structural and Multidisciplinary Optimization, 43(1), 1-16.
[25] Sigmund, O., & Maute, K., 2013, "Topology optimization approaches. Structural and Multidisciplinary Optimization," 48(6), 1031-1055.
[26] Sigmund, O., 1997, "On the design of compliant mechanisms using topology optimization," Journal of Structural Mechanics, 25(4), 493-524.
[27] Bruns, T. E., & Tortorelli, D. A., 2001, "Topology optimization of non-linear elastic structures and compliant mechanisms," Computer methods in applied mechanics and engineering, 190(26-27), 3443-3459.
[28] Bourdin, B., 2001, "Filters in topology optimization,".International Journal for Numerical Methods in Engineering, 50(9), 2143-2158.
[29] Guest, J. K., Prévost, J. H., & Belytschko, T., 2004, "Achieving minimum length scale in topology optimization using nodal design variables and projection functions," International journal for numerical methods in engineering, 61(2), 238-254.
[30] Xu, S., Cai, Y., & Cheng, G., 2010, "Volume preserving nonlinear density filter based on heaviside functions," Structural and Multidisciplinary Optimization, 41(4), 495-505.
[31] Michael O. V., & Jim D., 2017, "Image Quality Assessment Techniques Show Improved Training and Evaluation of Autoencoder Generative Adversarial Networks," *arXiv:1708.02237 [cs]*, Aug.
[32] Murat K., Christopher S., Alexandros G. D., & Sriram V., 2017, "CausalGAN: Learning Causal Implicit Generative Models with Adversarial Training," *arXiv:1709.02023 [cs]*, Sep
[33] Zuo, Z. H., Xie, Y. M., & Huang, X., 2011, "Reinventing the wheel," Journal of Mechanical Design, 133(2), 024502.
[34] Xiao, D., Zhang, H., Liu, X., He, T., & Shan, Y., 2014, "Novel steel wheel design based on multi-objective topology optimization," Journal of Mechanical Science and Technology, 28(3), 1007-1016.